

Article

# Limitations of Water Resources to Crop Water Requirement in the Irrigation Districts along the Lower Reach of the Yellow River in China

Lei Liu , Jianqin Ma <sup>\*</sup>, Xiuping Hao and Qingyun Li

School of Water Conservancy, North China University of Water Resources and Electric Power,  
No.36 Beihuan RD., Zhengzhou 450011, China

\* Correspondence: majianqin@ncwu.edu.cn

Received: 24 July 2019; Accepted: 21 August 2019; Published: 28 August 2019



**Abstract:** To analyze the water-resource limitations for crops in irrigation districts along the lower reach of the Yellow River, we used the single-crop coefficient method provided by FAO-56 to analyze crop water demand (CWD) and irrigation water requirement (IWR) for the main crops (winter wheat, summer maize, and cotton) from 1971 to 2015. The impact of climate threats on IWR was then quantified based on the standardized precipitation evapotranspiration index (SPEI), following which the conflicts between water demand and water supply were analyzed. The results show that about 75.4% of the total annual IWR volume is concentrated from March to June. Winter wheat is the largest water consumer; it used an average of 67.9% of the total IWR volume. The study area faced severe water scarcity, and severe water deficits occurred mainly between March and June, which is consistent with the occurrence of drought. With the runoff from the Yellow River Basin further decreasing in the future, the water supply is expected to become more limited. IWR is negatively correlated with the SPEI. Based on the relationship between SPEI and IWR, the water allocation for irrigation can be planned at different timescales to meet the CWD of different crops.

**Keywords:** crop water demand; irrigation water requirement; standardized precipitation evapotranspiration index; irrigation districts

---

## 1. Introduction

Irrigation districts along the lower reach of the Yellow River is an important grain and cotton base of China. Given the uneven spatial and temporal distribution of precipitation, irrigation is important to guarantee the high and stable crop production in this area.

Irrigation-water sources in this study area include local surface water, groundwater, and water from the Yellow River. However, local surface water and groundwater are in short supply and are difficult to use, so water from the Yellow River is the most important irrigation-water source for crop production. With the impact of climate change and human activities, the supply of water from the Yellow River is expected to become increasingly limited in the future. The observed mean annual runoff at Huayuankou Hydrological Station from 2001 to 2010 was less than 45.6% of that from 1956 to 1979 [1]. Due to economic development and population growth, more and more water withdrawn from the Yellow River is diverted from agriculture to meet the increased water needs of industrialized and urbanized areas. The proportion of the water withdrawn from the Yellow River for agriculture has thus declined since 2001 (Figure 1), which has worsened the water shortage for crop growth in the study area. Furthermore, runoff in the Yellow River Basin will be further reduced under the impact of climate change in the future [1], which will inevitably worsen the conflict between water demand and water supply and will constitute a strong threat to the safety of crop production in the study area. Thus,

to relieve the water shortage in the region and ensure both high and stable crop production in China, we need to understand the changes in crop water demand (CWD) and irrigation water requirement (IWR) of the main crops under the impacts of climate change.

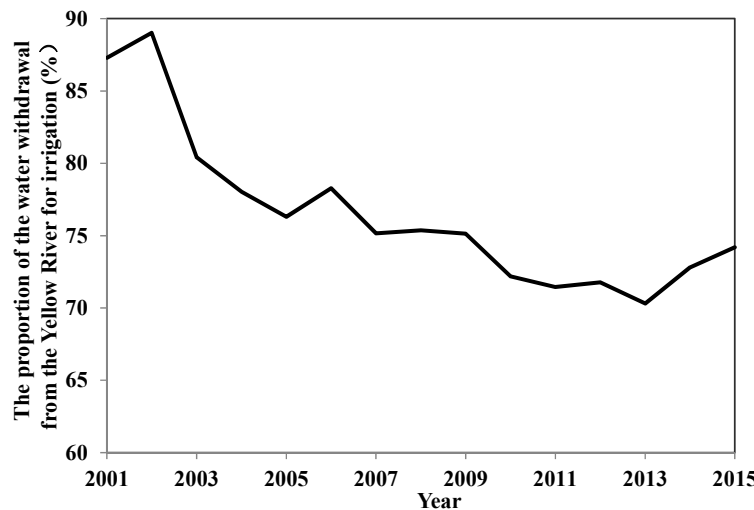


**Figure 1.** Interannual variations in the water withdrawn from the Yellow River for agriculture irrigation in the study area (data from the Yellow River Water Resources Bulletin of the Yellow River Conservancy Commission of the Ministry of Water Resources [2]).

CWD is affected by crop potential evapotranspiration (PET). When precipitation cannot satisfy CWD, crops experience water stress. The level of water stress is controlled by PET and precipitation. Thus, in this study, we chose to use the standardized precipitation evapotranspiration index (SPEI), which is calculated based on precipitation and PET, to quantify how climate change affects the crop water productivity. The SPEI was proposed by Vicente-Serrano [3] and has been widely used as a drought index to detect and monitor agricultural droughts at different timescales [4–9]. Studies of the variation of SPEI are helpful in defining drought levels for different crop growth periods and for properly planning the irrigation-water resources according to the temporal distribution of the IWR of the various crops.

The single-crop coefficient method provided by FAO-56 is widely used to calculate the IWR. This method first calculates the CWD by multiplying PET by the crop coefficient and then uses the difference between CWD and the effective precipitation as the IWR [8–14]. PET is usually calculated by using the Penman–Monteith equation recommended by the Food and Agriculture Organization (FAO) [15]. Although the crop coefficient, which is related to the crop type, crop growth stage, climate, and soil, is given by the FAO, it assumes standard conditions and usually should be adjusted according to the local meteorological conditions (wind speed and humidity), soil type, mean plant height, time intervals, magnitude of precipitation and irrigation, and the evaporation power of the atmosphere [12,15–17].

The objectives of this study are as follows: (1) to quantify the temporal changes of crop water demand and irrigation water requirement under the impact of climate change; and, (2) to comprehensively analyze the conflict between water supply and irrigation water requirement.

## 2. Materials and Methods

### 2.1. The Study Area

Irrigation districts along the lower reach of the Yellow River lie between latitude 34°12' and 38°02' N and longitude 113°24' and 118°59' E. The study area is in the Huang-Huai-Hai (HHH) plain [18] (Figure 2), which has a warm-temperate and semi-humid continental monsoon climate. The average

annual precipitation was 600 mm, with 70% falling from June to September, and the average annual temperature was 13.5 °C.

Winter wheat, summer maize, and cotton are the predominant crops in this region. In 2015, the total planting area of farm crops in the study area was  $818 \times 10^4$  ha. The planting area of winter wheat, summer maize, and cotton covers about 40.4%, 29.0%, and 5.3% of the total planting area, respectively [19,20].

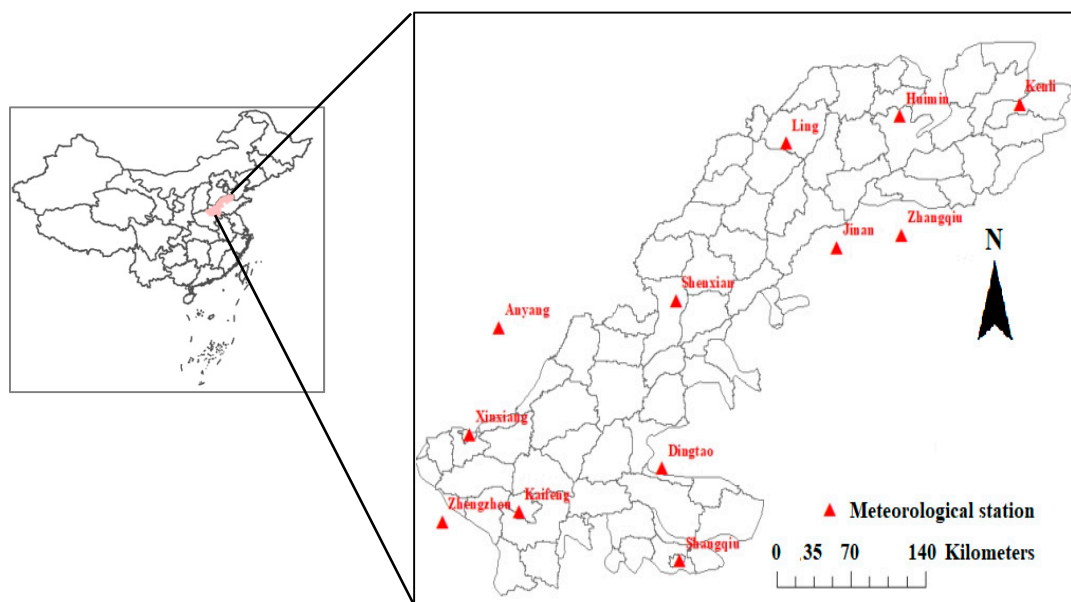


**Figure 2.** Study area and location of meteorological stations.

## 2.2. Data

Daily meteorological data from twelve national meteorological stations were used in this study; the locations of these stations are shown in Figure 2. The historical records of daily meteorological data from 1971 to 2015 were collected from the National Meteorological Information Centre of the China Meteorological Administration (<http://data.cma.cn>). The data included the maximum and minimum temperature, precipitation, sunshine hours, wind speed, and relative humidity.

## 2.3. Methods

### 2.3.1. Calculation of CWD and IWR

The CWD is calculated based on the single crop coefficient given by FAO-56:

$$ET_c = K_c \times PET \quad (1)$$

where  $ET_c$  is the CWD;  $PET$  is the potential evapotranspiration, which is estimated by the Penman–Monteith equation recommended by FAO;  $K_c$  is the crop coefficient, which is generalized into three values:  $K_{cini}$  for the initial growing stage,  $K_{cmid}$  for midseason, and  $K_{cend}$  for the end stage. The FAO has provided  $K_c$  values under standard conditions for different crops. These recommended  $K_c$  values should be modified according to the actual meteorological conditions [15]. Based on field-weighting lysimeter data, Liu and Luo [21] estimated  $K_c$  values during the initial, development, midseason, and end stages of winter wheat and summer maize in North China. This study uses the  $K_c$  values for the corresponding stages given by Liu and Luo [21]: the  $K_c$  values during the initial, development, midseason, and end stages for winter wheat were 0.80, 1.15, 1.25, and 0.95, and for summer maize were 0.90, 0.95, 1.25, and 1.00, respectively. Ma et al. [22] modified the cotton  $K_c$  values recommended by the FAO for the various cotton-planting regions of China. We used the modified  $K_c$

values for cotton in the HHH cotton-planting region from the study of Ma et al. [22]: the  $K_c$  values for the initial, midseason, and end stage were 0.35, 1.20, and 0.60, respectively.

The  $IWR$  can be calculated based on the difference between the CWD and the effective precipitation [23,24]:

$$IWR = ET_c - P_e \quad (2)$$

where  $ET_c$  is the CWD,  $P_e$  is the effective precipitation, and  $IWR$  is the irrigation water requirement. The effective precipitation is calculated by using

$$P_e = \alpha \times P \quad (3)$$

where  $P$  is the precipitation,  $P_e$  is the effective precipitation, and  $\alpha$  is the effective utilization coefficient of precipitation. In this study, we use  $\alpha = 0.80$  because of the large study area with different types of land use and soil types.

Understanding the variations in CWD and  $IWR$  for different crop growth periods is helpful for water-resource allocation for irrigation. In this study, the whole growth stage of different crops was divided into different growth periods. Winter wheat is usually planted in early or middle October and harvested in early June of the following year. Its growth season was divided into three growth stages: (i) the sowing-to-tillering stage (BBCH 00-29), (ii) the over-wintering stage, and (iii) the greening-to-maturity stage (BBCH 31-97). The growth season of summer maize usually extends from early or mid-June to mid or late September and was divided into four growth stages: (i) the sowing-to-jointing stage (BBCH 00-30), (ii) the jointing-to-heading stage (BBCH 30-51), (iii) the heading-to-milk stage (BBCH 51-73), and (iv) the milk-to-maturity stage (BBCH 73-97). The growth season of cotton is usually from mid-April to mid or late October and was divided into three growth stages: (i) the sowing-to-flowering stage (BBCH 00-60), (ii) the flowering-to-boll-opening stage (BBCH 60-81), and (iii) the boll-opening-to-maturity stage (BBCH 81-97).

### 2.3.2. Standardized Precipitation Evapotranspiration Index (SPEI)

In the study of Vicente-Serrano et al. [3], the estimate of SPEI was based on the difference between monthly precipitation and PET. In this study, we followed the computational procedures proposed by Vicente-Serrano et al. [3] to calculate the SPEI.

The first step is to calculate the PET, which was done by using the Thornthwaite method in the study of Vicente-Serrano et al. [3]. The PET is easy to calculate by the Thornthwaite method [25] because it uses only the monthly average temperature and latitude as the input data. However, the PET in China is not only affected by temperature but also controlled by other climate factors, such as wind speed, relative humidity, and solar radiation [26]. Furthermore, PET calculated by the Thornthwaite method usually results in an overestimate [27]. Therefore, the FAO-56 Penman–Monteith equation, which combines the aerodynamics and radiative climate factors and is usually adopted as a standard method to compute PET, is used herein because it provides more accurate results [28–31].

The second step is to compute the difference  $D_i$  between the monthly precipitation and monthly PET for month  $i$ :

$$D_i = P_i - PET_i \quad (4)$$

where  $D_i$  is the difference between the monthly precipitation and monthly PET,  $P_i$  is the monthly precipitation, and  $PET_i$  is the monthly CWD.

The third step is to determine the accumulation of  $D_i$  over different timescales, and the fourth step is to standardize  $D_i$  into a three-parameter log-logistic probability distribution to obtain the SPEI:

$$F(x) = \left[ 1 + \left( \frac{\alpha}{x - \gamma} \right)^{\beta} \right]^{-1} \quad (5)$$

$$P = 1 - F(x) \quad (6)$$

where  $F(x)$  is the probability function of the log-logistic distribution for the  $D$  series;  $\alpha$ ,  $\beta$ , and  $\gamma$  are the scale, shape, and origin parameters, which can be obtained by using the L-moment procedure [3,32], and  $P$  is the probability of exceeding a determined  $D$  value.

When  $P \leq 0.5$ ,

$$W = \sqrt{-2 \ln P} \quad (7)$$

$$SPEI = W - \frac{2.515517 + 0.802853W + 0.010328W^2}{1 + 1.432788W + 0.189269W^2 + 0.001308W^3} \quad (8)$$

when  $P > 0.5$ ,

$$W = \sqrt{-2 \ln(1 - P)} \quad (9)$$

$$SPEI = \frac{2.515517 + 0.802853W + 0.010328W^2}{1 + 1.432788W + 0.189269W^2 + 0.001308W^3} - W \quad (10)$$

where  $W$  in Equations (7)–(10) is the probability-weighted moment.

SPEI can be estimated at different timescales, such as 1, 3, 6, and 12 months. For example, the 3-month SPEI in May ( $SPEI_{3-5}$ ) means that the estimation of SPEI is based on the sum of monthly precipitation and PET of May, April, and March.

The SPEI is classified into five levels according to the China national standard Grades of Meteorological Drought (GB/T 20481-2017) [33]: no drought ( $SPEI > -0.5$ ), light drought ( $-1.0 < SPEI \leq -0.5$ ), moderate drought ( $-1.5 < SPEI \leq -1.0$ ), severe drought ( $-2.0 < SPEI \leq -1.5$ ), and extreme drought ( $SPEI \leq -2.0$ ).

To properly plan the irrigation water resources, drought characteristics should be analyzed in different growth stages of crops based on the above classification of the whole growth stage for the given crops. For winter wheat, the drought characteristics during the first growth stage were assessed based on the 2-month SPEI of November, the second was the 3-month SPEI of February, and the third was the 4-month SPEI of June. For the whole growth season, they were assessed based on the 9-month SPEI of June.

For summer maize, drought characteristics during each growth stage were assessed based on the 1-month SPEI series from June to September. Drought characteristics during the whole growth season of summer maize were assessed based on the 4-month SPEI of September.

For cotton, the drought characteristics of each growth stage were assessed based on the 3-month SPEI of June, 2-month SPEI of August, and 2-month SPEI of October. For the whole growth season of cotton, they were assessed based on the 7-month SPEI of October.

### 2.3.3. Temporal and Trends Analysis

The rank-based nonparametric Mann–Kendall (MK) test [34,35], which detects the trends of non-normally distributed data and is strongly recommended by the World Meteorological Organization [36], was used to test the significance of the trends of the CWD and IWR on different timescales. Sen's slope estimator  $\beta$  [37], which is a slope-based method and is closely related to the Mann–Kendall test, was used to quantify the magnitude of the trends, and the Pearson correlation coefficient was used to analyze the influence of climate threats on the IWR at the 1% significance level.

Finally, the inverse-distance weighting method was used to calculate the regional average value of the CWD and IWR of different crops and the SPEI on different timescales in the study area.

## 3. Results and Analysis

### 3.1. Analysis of Trends for Crop Water Demand and Irrigation Water Requirements

Tables 1–3 present the results of the trend analysis for the CWD and IWR for winter wheat, summer maize, and cotton, respectively, from 1971 to 2015.

For winter wheat, the mean annual CWD varied from 404 to 559 mm with an average of 487 mm ( $SD = 33$  mm), and the mean IWR for winter wheat varied from 168 to 452 mm with an average of 322 mm ( $SD = 65$  mm) (Table 1). During the whole growth season, the CWD tended to decrease at the rate of 0.5 mm/decade from 1971 to 2015, but this trend was not significant. No significant increasing trends appeared in the sowing-to-tillering stage (BBCH 00-29) and over-wintering stage. However, during the greening-to-maturity stage (BBCH 31-97), the CWD decreased insignificantly at a rate of 4.3 mm/decade, which may be the main contribution to the decreasing trend of the whole growth season for CWD during this growth stage being the most and it accounts for 75.2% of the CWD for the whole growth season. The IWR for the whole growth season decreased insignificantly at a rate of 7.1 mm/decade. For the changes of different growth stages, the IWR during the sowing-to-tillering period (BBCH 00-29) and the greening-to-maturity stage (BBCH 31-97) tended to decrease as well, although not significantly, and increased insignificantly at a rate of 0.5 mm/decade during the over-wintering period.

**Table 1.** Average CWD, IWR, MK trends and Sen's slope estimator  $\beta$  during the different growth stages of winter wheat.

Growth Stage		CWD	IWR
Sowing to tillering (BBCH 00-29)	Mean	54.12	20.13
	Z	0.56	-0.89
	$\beta$	0.05	-0.14
Over-wintering	Mean	67.33	45.48
	Z	0.29	0.17
	$\beta$	0.04	0.05
Greening to maturity (BBCH 31-97)	Mean	366.05	256.49
	Z	-1.18	-0.75
	$\beta$	-0.43	-0.55
Whole growth period (BBCH 00-97)	Mean	486.58	321.53
	Z	-0.27	-0.88
	$\beta$	-0.09	-0.71

Note: CWD means crop water demand; IWR means irrigation water requirement; MK means Mann-Kendall.

For summer maize, the mean annual CWD varied from 302 to 417 mm with an average of 343 mm ( $SD = 26$  mm), and the mean annual IWR varied from 114 to 328 mm with an average of 213 mm ( $SD = 46$  mm) (Table 2). The CWD during the whole growth stage decreased significantly at a rate of 8.8 mm/decade. Similar decreasing trends also occurred during different growth stages; even significant downward trends appeared during the sowing-to-jointing stage (BBCH 00-30) and the heading-to-milk stage (BBCH 51-73). The IWR decreased significantly at a rate of 21.7 mm/decade over the whole growth season, and significant decreasing trends that exceeded that of the CWD also occurred during the different growth periods of summer maize. From 1971 to 2015, the IWR decreased significantly at rates of 4.9, 6.2, 7.4, and 3.9 mm/decade during the different growth periods, respectively.

For cotton, the mean annual CWD varied from 482 to 628 mm with an average of 541 mm ( $SD = 34$  mm), and the mean annual IWR varied from 80 to 372 mm with an average of 185 mm ( $SD = 67$  mm) (Table 3). The CWD of the whole growth season for cotton decreased significantly at a rate of 11.9 mm/decade, which was similar to the trend for summer maize. Decreasing trends also occurred during the different growth stages; in particular, the CWD decreased significantly at a rate of 5.3 and 6.0 mm/decade during the sowing-to-flowering stage (BBCH 00-60) and the flowering-to-boll opening stage (BBCH 60-81), respectively. The IWR decreased significantly at a rate of 14.9 mm/decade over the whole growth season and at a rate of 11 mm/decade during the sowing-to-flowering stage (BBCH 00-60). During the flowering-to-boll-opening stage (BBCH 60-81) and the boll-opening-to-maturity stage (BBCH 60-81), the IWR decreased as well, but not significantly.

**Table 2.** Average CWD, IWR, MK trends and Sen's slope estimator  $\beta$  during the different growth stages of summer maize.

Growth Stage		CWD	IWR
Sowing to jointing (BBCH 00-30)	Mean	73.09	51.21
	Z	-2.08 **	-2.55 *
	$\beta$	-0.23	-0.49
Jointing to heading (BBCH 30-51)	Mean	101.74	44.59
	Z	-1.11	-2.77 *
	$\beta$	-0.12	-0.62
Heading to milk (BBCH 51-73)	Mean	106.37	65.05
	Z	-2.49 *	-3.10 *
	$\beta$	-0.34	-0.74
Milk to maturity (BBCH 73-97)	Mean	62.28	46.23
	Z	-1.52	-2.71 *
	$\beta$	-0.14	-0.39
Whole growth period (BBCH 00-97)	Mean	343.47	213.42
	Z	-3.14 *	-3.98 *
	$\beta$	-0.88	-2.17

Note: CWD means crop water demand; IWR means irrigation water requirement; MK means Mann–Kendall; \* represents significant at the 0.01 level; \*\* represents significant at the 0.05 level.

**Table 3.** Average CWD, IWR, MK trends and Sen's slope estimator  $\beta$  during the different growth stages of cotton.

Growth Stage		CWD	IWR
Sowing to flowering (BBCH 00-60)	Mean	208.29	103.73
	Z	-3.04 *	-2.02 **
	$\beta$	-0.53	-1.1
Flowering to boll opening (BBCH 60-81)	Mean	238.06	42.57
	Z	-2.47 *	-0.98
	$\beta$	-0.6	-0.26
Boll opening to maturity (BBCH 81-97)	Mean	95.09	38.63
	Z	-1.46	-0.18
	$\beta$	-0.18	-0.03
Whole growth period (BBCH 00-97)	Mean	541.44	184.92
	Z	-3.16 *	-2.04 **
	$\beta$	-1.19	-1.49

Note: CWD means crop water demand; IWR means irrigation water requirement; MK means Mann–Kendall; \* represents significant at the 0.01 level; \*\* represents significant at the 0.05 level.

### 3.2. Temporal Variation of Irrigation Water Requirement

To analysis the intra-annual and interannual variation in IWRs and the climate threats to IWRs, we calculated the IWR volume based on the cropping area in 2000. Figure 3 shows the interannual variation of IWR volume for winter wheat, summer maize, and cotton from 1971 to 2015. The average annual total IWR volume varied from  $97.0 \times 10^8$  to  $210.7 \times 10^8 \text{ m}^3$ , with an average of  $146.9 \times 10^8 \text{ m}^3$  ( $SD = 25.2 \times 10^8 \text{ m}^3$ ). Precipitation was negatively correlated with total IWR volume ( $r = -0.61$ ,  $p < 0.01$ ). The total IWR volume peaked in 1981 with a 91% annual precipitation frequency, and was the lowest in 2003 with a 2% annual precipitation frequency. Of these three crops, winter wheat, which had the largest planting area, was the largest water consumer, accounting for an average of 67.9% of the total IWR volume. Although the CWD of summer maize (cotton) is the lowest (highest), the IWR volume for summer maize exceeds that of cotton because summer maize had a larger planting area than cotton.

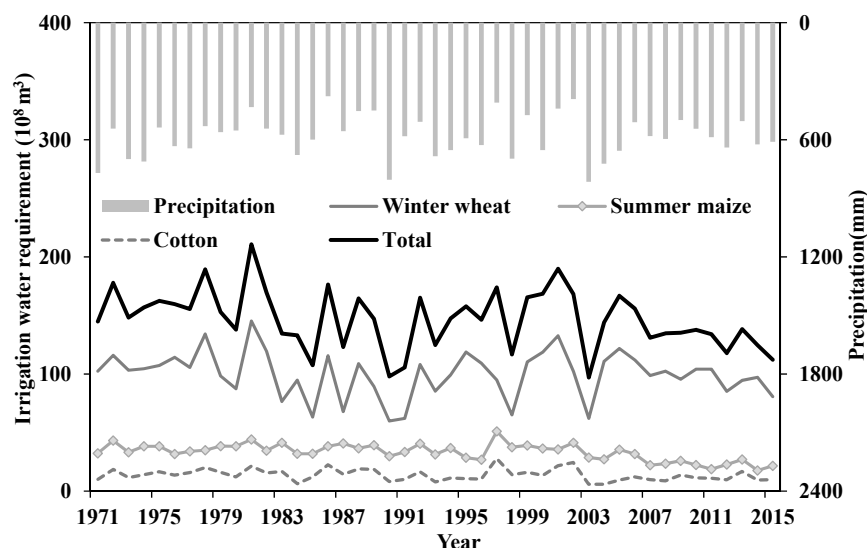


**Figure 3.** Interannual variation of IWR volume and precipitation from 1971 to 2015.

Figure 4. presents the intra-annual variation of IWR volume for winter wheat, summer maize, and cotton from 1971 to 2015. Most of the IWR volume was concentrated from March to June and the IWR volume during this period accounted for 75.4% of the total annual IWR volume of the study area. March to May was the rapid growth stage of winter wheat and the IWR volume of winter wheat during this growth period accounted for 64.9% of the total annual IWR volume from March to June. Furthermore, cotton was sowed in April, and the IWR volume of cotton in April was much less than that of winter wheat. The IWR volume gradually decreased after May. In June, although winter wheat entered its maturity stage and its IWR volume was much less than in March, April, and May, summer maize was sowed after the winter wheat was harvested and it needed sufficient water to ensure its emergence of seedlings in June which had less rainfall. Cotton entered its budding stage in June and also needed sufficient water to satisfy its high water requirements (its IWR volume in June accounted for 15.4% of the total annual IWR for cotton). Starting in July, the IWR volume decreased and most of the rainfall was concentrated in July and August, so the CWD of summer maize and cotton could almost have been satisfied by rainfall (no irrigation water was needed when rainfall was abundant). Starting in September, the IWR volume gradually decreased, for summer maize and cotton gradually entered their maturity stage in September to October, respectively. In addition, winter wheat was sowed in October and entered its initial growth stages in November and December, which resulted in a much smaller IWR volume from October to December compared with other months.

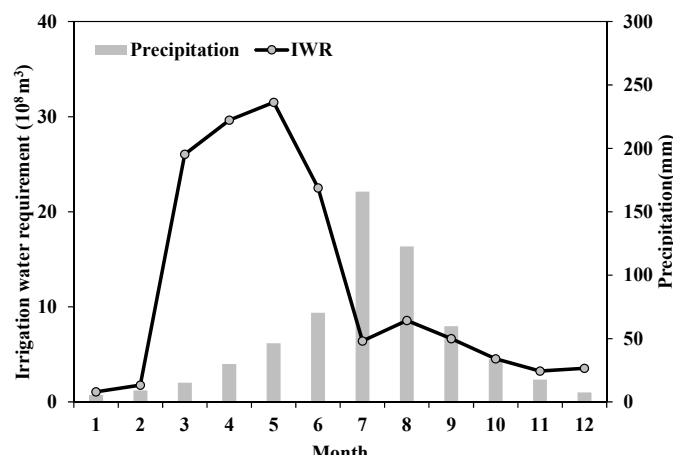


**Figure 4.** Average monthly IWR volume and precipitation from 1969 to 2015.

### 3.3. Drought Analysis

As can be seen from Figure 5a, the SPEI values for the whole growth period of winter wheat were all negative and 39 out of 45 years had SPEI values less than  $-0.5$ , which means that winter wheat tended to suffer from drought in the study area. During the whole growth period of winter wheat, drought afflicted the region with a probability of 93.6%, with light drought occurring at a ratio of 25.5%, moderate drought 27.7%, severe drought 25.5%, and extreme drought 14.9%. According to the interannual variability of the SPEI values in different growth stages, light drought occasionally occurred during the growth stage from October to November (Figure 5b) and from December to February (Figure 5c). Drought during the stage from March to June occurred frequently with a high probability of 91.5% (Figure 5d), especially severe drought and extreme drought occurred at a ratio of 19.1% and 27.7%, respectively.

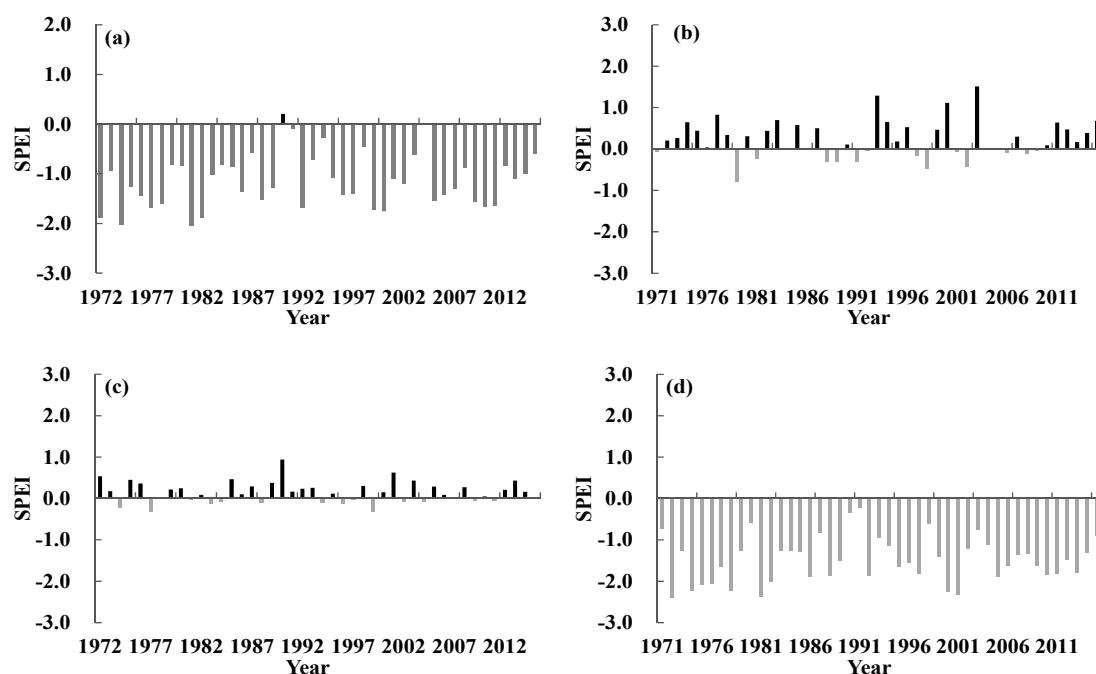


**Figure 5.** Interannual variability of SPEI during growth stage of winter wheat from 1971 to 2015: (a) whole growth period; (b) October to November; (c) December to February; and (d) March to June.

Almost no droughts occurred during the whole growth period of summer maize, with the exception that only 3 years had a SPEI value less than  $-0.5$  (Figure 6a). According to the interannual variability of SPEI values in different growth stages, drought often occurred in June (Figure 6b): light drought occurred at a ratio of 21.3%, moderate drought 17.0%, severe drought 10.6%, and extreme drought 14.9%. July and August were dominated by a humid climate and most of the SPEI values for these two months were positive, even though there were four or five years with negative SPEIs, only light drought occurred occasionally during these two months (Figure 6c,d). In September, 16 years had negative SPEI values, but only the SPEI values in 1981 and 1998 were less than  $-1.0$  (Figure 6e). The occurrence probability of light drought was 10.6%, and for moderate drought it was 4.3%.

The occurrence probability of drought during the whole growth period of cotton was not high. Although 18 out of 45 years had negative SPEIs, only 8 years had SPEIs less than  $-0.5$  (Figure 7a). Drought during the growth period of cotton occurred frequently from April to June (Figure 7b): the occurrence probability of light drought was 25.5%, moderate drought 21.3%, severe drought 25.5%, and extreme drought 21.3%. The growth stage from July to August was dominated by a humid climate, and nearly all SPEIs were positive (Figure 7c). During the stage from September to October, nearly half of the SPEIs were negative, but only the SPEI of 1998 was less than  $-1.0$  (Figure 7d).

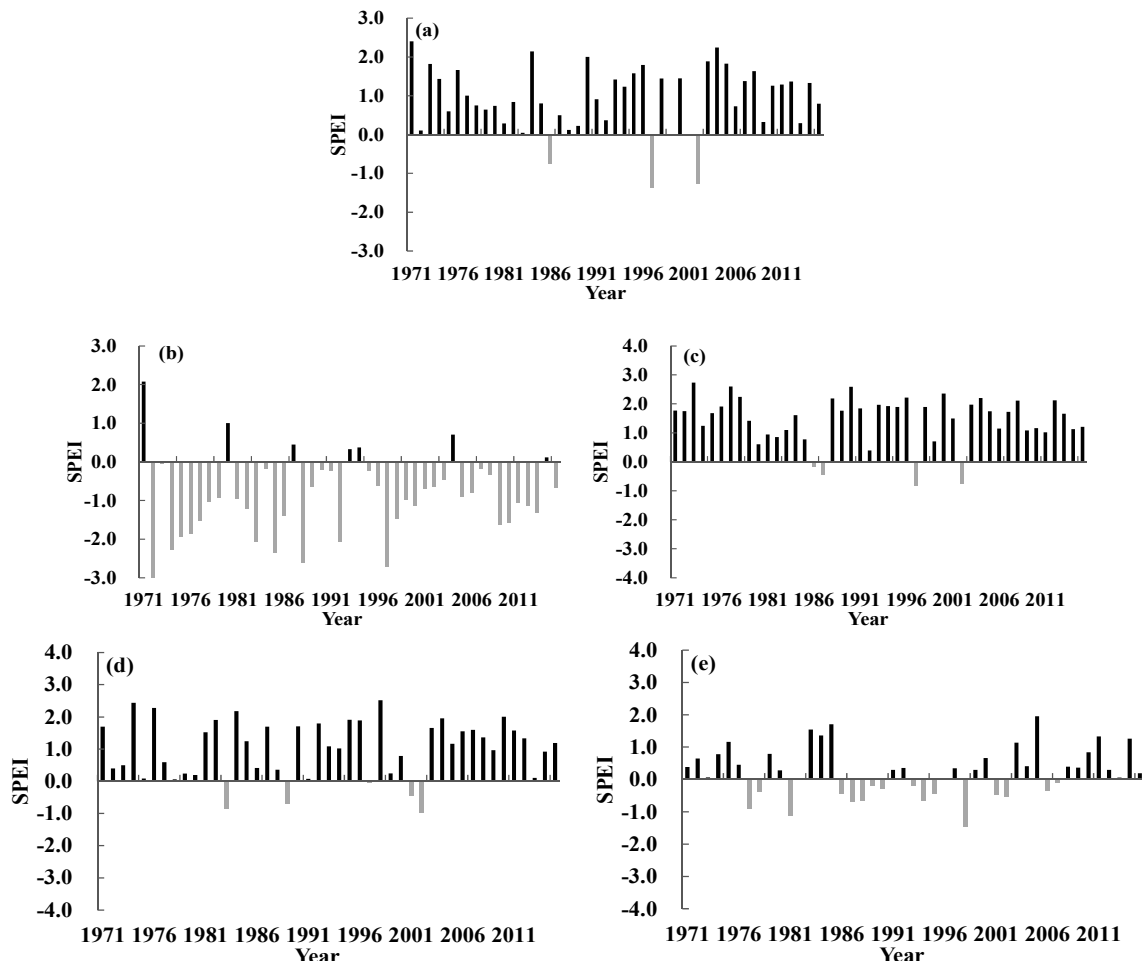


**Figure 6.** Interannual variability of SPEI during growth stage of summer maize from 1971 to 2015: (a) whole growth period; (b) June; (c) July; (d) August; and (e) September.

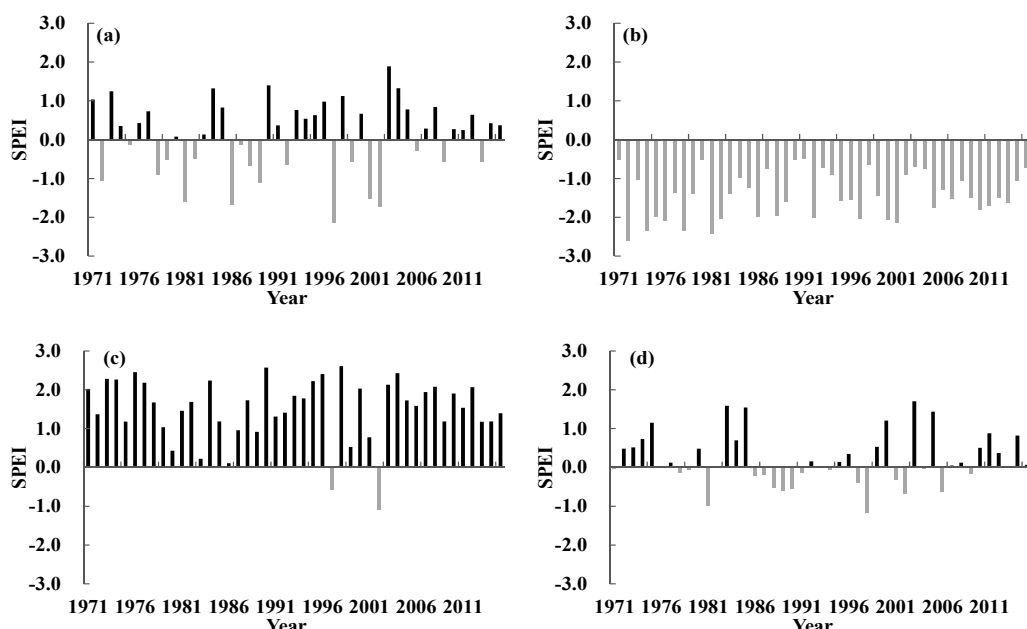


**Figure 7.** Interannual variability of SPEI during growth stage of cotton from 1971 to 2015: (a) whole growth period; (b) April to June; (c) July to August; and (d) September to October.

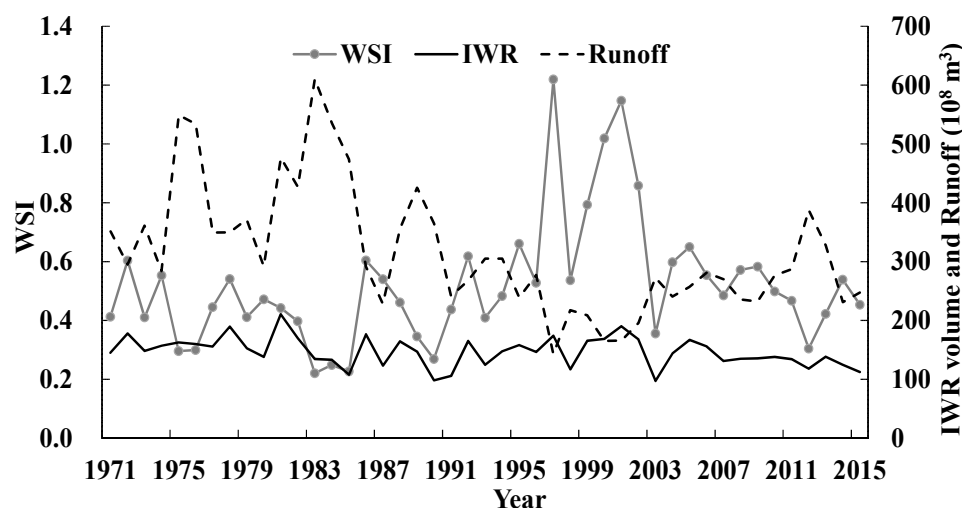
## 4. Discussion

### 4.1. Limitation of Water Resources for Irrigation Water Requirement

Huayuankou Hydrological Station is located in the uppermost part of the Yellow River within the study area. Thus, we used the annual and seasonal variation in runoff at the Huayuankou Hydrological Station to analyze the water supply situation for winter wheat, summer maize, and cotton.

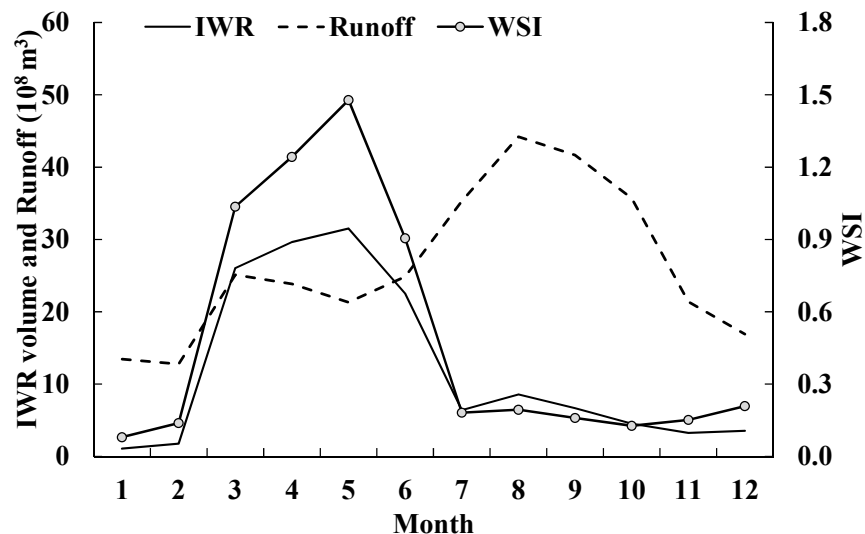
The water scarcity index (WSI) is defined by Raskin [38] as the ratio of IWR to runoff (IWR/R) and was used to evaluate the water scarcity in the study area. The WSI from 1971 to 2015 varied from 0.22 to 1.22, with an average of 0.52 (Figure 8), which means that the study area suffered from severe water scarcity. According to the mean annual WSI, the study area faced moderate scarcity for 10 years ( $0.2 \leq \text{WSI} < 0.4$ ) and severe scarcity for 35 years ( $\text{WSI} > 0.4$ ). The WSI in 1997, 2000, and 2001 even exceeded 1.0. Although the highest IWR volume was  $210.7 \times 10^8 \text{ m}^3$  and occurred in 1981, the WSI was 0.44. However, the IWR volumes in 1997, 2000, and 2001 were less than in 1981, and the WSIs for these three years exceeded 1.0, which might be due to the drastic reduction of runoff from the Yellow River (Figure 8).

WSI was different in different decades. In the period from 1971 to 1979, the average WSI was 0.44, and it was 0.40 from 1980 to 1989, 0.60 from 1990 to 1999, and 0.69 from 2000 to 2009, which was the highest WSI. Although the WSI dropped a bit since 2010 and the WSI was 0.44, the study area will still face severe water scarcity because there is an increasing trend in WSI from 1971 to 2015, which is significant at the 0.05 level.



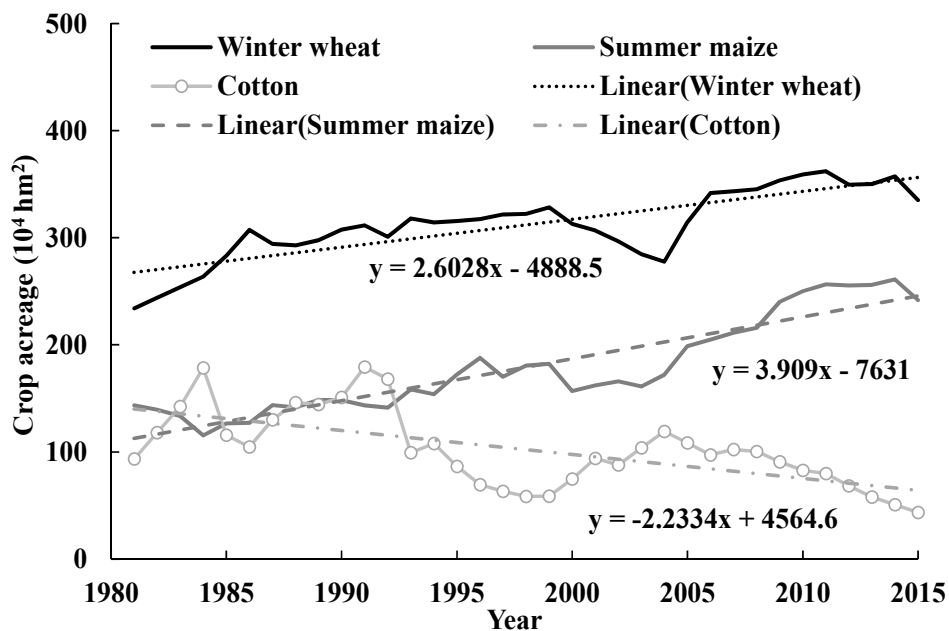
**Figure 8.** Annual variation in water scarcity index (WSI), IWR volume, and runoff at the Huayuankou Hydrological Station from 1971 to 2015.

Figure 9 compares the monthly IWR with runoff. Because of the seasonal distribution of the runoff and of the IWR, severe water deficit often occurred in the study area in spring (from March to May) because the IWR exceeded the runoff during these three months and the WSI exceeded 1.0. March to May is the key stage for the production of winter wheat, so water deficit during this period can significantly reduce the yield of winter wheat. Zhang et al. [39] reported that drought occurring from March to May could reduce the winter wheat yield by 3.93%–24.84%. Although the IWR in June was less than the runoff, the study area often encountered severe water scarcity, for the annual average WSI in June was 0.91. June is the seeding stage of summer maize and irrigation during this stage is the foundation for high production of summer maize [40]. April to June is the period for cotton seeding and budding, so severe water deficit during this period also could reduce the growth and production of cotton [41]. During the other months, no water shortages occurred because the IWR was less than the runoff and the WSI was often less than 0.2.



**Figure 9.** Monthly variations of WSI, IWR volume, and runoff at the Huayuankou Hydrological Station.

To analyze how climate threats may affect IWR, we analyzed the above results without considering changes in crop acreage. In fact, the acreage of different crops changes from year to year. For example, the acreage of winter wheat and summer maize increased significantly from 1981 to 2015, and the acreage of cotton decreased (Figure 10). The total IWR volume tended to increase from 1981 to 2015 when considering changes in crop acreage, whereas it tended to decrease when considering only climate change (Figure 11). Thus, in the study area, the water supply situation for irrigation was actually more severe than reported above.



**Figure 10.** Variation of acreage of different crops from 1981 to 2015 (crop acreage data from the Henan statistical yearbook from 1982 to 2016 and the Shandong statistical yearbook from 1982 to 2016 [19,20]).

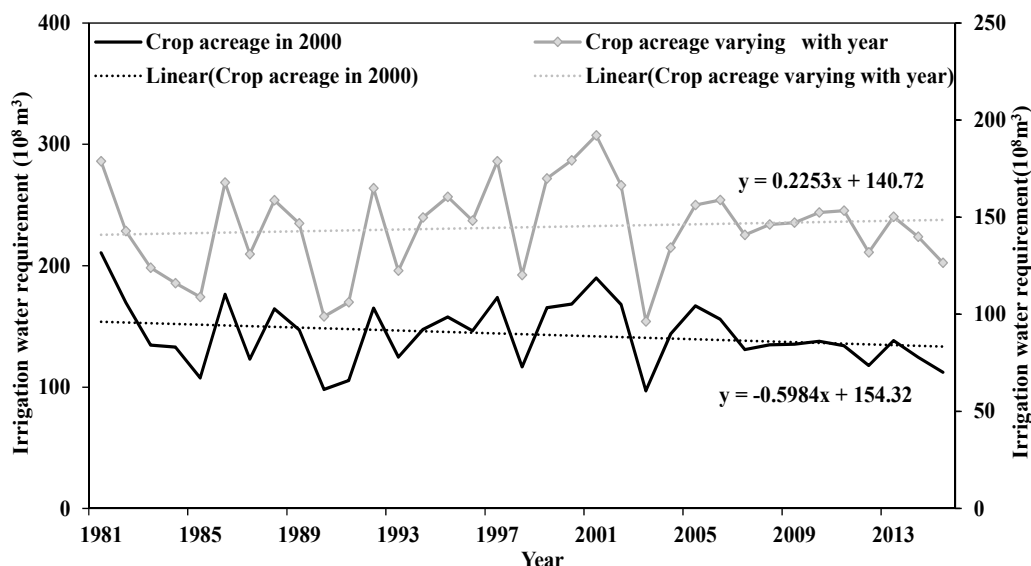


**Figure 11.** IWR volume with and without considering changes in crop acreage.

#### 4.2. Relationship between SPEI and IWR

The IWR of different crops was affected mostly by the CWD and precipitation [15,18]. Pirmoradian and Davatgar [42] used the reconnaissance drought index (RDI), which is based on the ratio of cumulative precipitation to cumulative PET, to analyze the drought conditions during the whole growth season of rice, and the IWR of rice was forecasted based on the relationship between IWR and RDI. The SPEI was estimated based on the difference between monthly precipitation and PET, so the relationship between SPEI and IWR can also be used to forecast the IWR of different crops.

With respect to duration of the different growing seasons of different crops in the study area, the SPEI was calculated at different timescales for the period from 1971 to 2015 (1 to 12 months) to analyze the relationship between SPEI and IWR based on the nonparametric Spearman's Rank Correlation test. The results show that the IWR is negatively correlated with the SPEI, which means that a higher SPEI corresponds to a lighter degree of drought, which translates into a smaller IWR.

According to the Spearman correlation analysis, the SPEI, which has the best correlation with IWR during the different growth stages of the different crops, was calculated; the corresponding correlation coefficients appear in Tables 4–6. To quantify the impact of climate threats on IWR, we use a regression analysis between the IWR and the most closely related SPEI based on SPSS. and the relationship between them is expressed by regression equations shown in Tables 4–6.

The relationship between the SPEI and IWR of different crops shows that the correlation coefficient between SPEI and IWR is most affected by the use of effective precipitation. The correlation coefficient between SPEI and IWR increased with increasing effective precipitation because an increase in effective precipitation makes it easier for the IWR to be affected by meteorological factors. The effective precipitation during the growth period of winter wheat was much less than that for summer maize and cotton, so the correlation coefficients between the SPEI and IWR of winter wheat are slightly less than that for summer maize and cotton.

**Table 4.** Relationship between SPEI and IWR during different growth stages of winter wheat.

Growth Stage	Regression Equation	Correlation Coefficient
Sowing to tillering	$IWR = -19.342 \times SPEI_{3-11} + 21.986$	-0.609
Over-wintering	$IWR = -18.268 \times SPEI_{3-12} + 12.600$	-0.671
Greening to maturity	$IWR = -64.861 \times SPEI_{2-12} + 282.376$	-0.464
Whole growth period	$IWR = -80.842 \times SPEI_{2-12} + 312.216$	-0.504

Note: SPEI in different regression equations is the SPEI which has the highest correlation with the IWR during the different growth stages of winter wheat.

**Table 5.** Relationship between SPEI and IWR during different growth stages of summer maize.

Growth Stage	Regression Equation	Correlation Coefficient
Sowing to jointing	IWR = $-10.485 \times \text{SPEI}_{1-6} + 27.408$	-0.668
Jointing to heading	IWR = $-22.672 \times \text{SPEI}_{2-7} + 61.166$	-0.833
Heading to milk	IWR = $-17.560 \times \text{SPEI}_{2-8} + 48.254$	-0.749
Milk to maturity	IWR = $-12.136 \times \text{SPEI}_{3-9} + 31.971$	-0.608
Whole growth period	IWR = $-52.267 \times \text{SPEI}_{3-8} + 173.339$	-0.886

Note: SPEI in different regression equations is the SPEI which has the highest correlation with the IWR during different growth stages of summer maize.

**Table 6.** Relationship between SPEI and IWR during different growth stages of cotton.

Growth Stage	Regression Equation	Correlation Coefficient
Sowing to Flowering	IWR = $-59.581 \times \text{SPEI}_{3-6} + 100.592$	-0.802
Flowering to Boll opening	IWR = $-26.881 \times \text{SPEI}_{3-8} + 76.216$	-0.826
Boll opening to Maturity	IWR = $-17.226 \times \text{SPEI}_{3-9} + 44.308$	-0.691
Whole growth period	IWR = $-47.936 \times \text{SPEI}_{5-8} + 269.344$	-0.830

Note: SPEI in different regression equations is the SPEI which has the highest correlation with the IWR during different growth stages of cotton.

For optimum water resources management, water allocation for irrigation should be preplanned. Given the relationship between the SPEI and IWR, the IWR of different crops can be estimated based on the SPEI. The SPEI can be calculated for different timescales, then the IWR of whole growth periods and even of different growth stages can be estimated, which provides useful information for water resources management. Thus, in the future, the SPEI can be predicted based on the mid- or long-term weather forecasts, following which the water allocation for irrigation can be planned on different timescales; for example, 1-month, 3-month, or 12-month, to meet the crop water requirement for the whole growth period or for different growth stages.

#### 4.3. Comparison with Similar Studies

In this work, we used the product of the crop coefficient and PET to estimate the CWD of winter wheat, summer maize, and cotton, and the IWR of these three crops were calculated based on the difference between the given CWD and the effective precipitation. To properly preplan the water allocation for irrigation, we analyzed herein the temporal variation of the CWD and IWR during the whole growth periods, and even during the different growth stages of different crops. However, most comparable studies concentrated on the CWD and IWR of the whole growth periods of different crops. For example, Wu et al. [10] studied the temporal variation of the IWR for the winter wheat–summer maize rotation system from 1982 to 2012 in the North China Plain and analyzed the IWR during the whole growth seasons of winter wheat and summer maize. Yang et al. [43] provided the temporal variation of the CWD and IWR under the effects of climate change over the whole growth season of summer maize in the HHH plain. Huang et al. [44] also studied the temporal variation of the CWD over the whole growth season of winter wheat, summer maize, and cotton in the HHH plain. Yet, there are few studies on the temporal variation of the CWD and IWR during the different growth stages of various crops.

The results of the present study show that the CWD and IWR of different crops decreased from 1971 to 2015. Thus, the results of our temporal analysis for the CWD and IWR of different crops are consistent with previous results. Zhou et al. [45] detected decreasing trends for the CWD of winter wheat, summer maize, and cotton from 1981 to 2010 in the Henan Province of China, and Zhang [46] reported that the IWR throughout the whole growth season of winter wheat and summer maize both decreased from 1966 to 2010 in the Yellow River Basin. Similar results were obtained in other studies [10,43,45].

The present study calculates the SPEI at different timescales to analyze the drought conditions of different crops. The results show that drought mainly occurred from March to June; that is, drought in this study area tended to occur mostly in the spring and early summer. Similar results were reported by previous studies. Li et al. [47] reported that drought occurred most frequently in spring (from March to May) in the Henan Province of China. Li. et al. [30] also reported that spring drought was the most predominant in the HHH plain, and Xue et al. [48] also reported that the occurrence probability of drought was the greatest in the early summer in the HHH plain.

## 5. Conclusions

This study quantifies the temporal changes of the CWD and IWR under the impact of climate change and analyzes the conflict between water supply and irrigation water demand to understand the water supply situation for the main crops in this area.

- (1) The CWD and IWR for winter wheat, summer maize, and cotton all decreased from 1971 to 2015. Based on the cropping area in 2000, the average annual total IWR volume was  $131.7 \times 10^8 \text{ m}^3$ , and precipitation was negatively correlated to total IWR volume. Most of the IWR volume was concentrated from March to May, accounting for 66.6% of the total annual IWR volume. Considering the water consumption and planting area of different crops, winter wheat was the largest water consumer, accounting for an average of 67.9% of the total IWR volume.
- (2) Winter wheat tended to be afflicted by drought during its whole growth period because droughts occurred frequently from March to June. However, drought almost never occurred over the whole growth period of summer maize. During the growth season of cotton, cotton tends to suffer from drought from April to June.
- (3) The water supply situation for winter wheat, summer maize, and cotton is severe. From 1971 to 2015, the study area faced moderate scarcity for 10 years and severe scarcity for 35 years. The results were analyzed without considering changes in the planting area of different crops. In fact, given the increase in the total planting area of winter wheat, summer maize, and cotton, the total IWR volume since 1981 tended to increase, which means that, given the decreasing runoff from the Yellow River Basin expected in the future, the water supply situation will be even more severe.
- (4) Severe water deficit occurred mainly from March to June, which is consistent with the high occurrence of drought during these months. No water shortage occurred during the other months. To ensure the safe growth of different crops and make the best use of water resources, water allocation for irrigation during different growth periods can be preplanned based on the relationship between the SPEI and IWR, which would allow the water deficit to be satisfied through reservoir regulation and storage.

**Author Contributions:** Conceptualization, L.L. and J.M.; Data curation, L.L., X.H., and Q.L.; Formal analysis, L.L.; Methodology, J.M.; Writing—original draft, L.L.; Writing—review & editing, X.H. and Q.L.

**Funding:** This research was financially supported by the National Natural Science Foundation of China (Grant No. 41601019), the Program for Science & Technology Innovation Talents in Universities of Henan Province (Grant No. 15HASTIT046), the Science and Technology Project of Henan Province (Grant No. 152102110095) and the Key Scientific Research Project of Henan Province Universities (Grant No. 15A570008).

**Conflicts of Interest:** The authors declare no conflict of interest.

## References

1. Hu, C.; Wang, J.; Chai, X.; Guan, X. Research advances of impact of climate change on runoff of the Yellow River Basin. *Meteorol. Environ. Sci.* **2013**, *36*, 57–65. (In Chinese)
2. Yellow River Conservancy Commission of the Ministry of Water Resources. *Yellow River Water Resources Bulletin*; Yellow River Conservancy Commission of the Ministry of Water Resources: Zhengzhou, China, 2001–2015.

3. Vicente-Serrano, S.M.; Beguería, S.; López-Moreno, J.I. A Multiscalar Drought Index Sensitive to Global Warming: The Standardized Precipitation Evapotranspiration Index. *J. Clim.* **2010**, *23*, 1696–1718. [[CrossRef](#)]
4. Potopová, V.; Štěpánek, P.; Možný, M.; Türkott, L.; Soukup, J. Performance of the standardised precipitation evapotranspiration index at various lags for agricultural drought risk assessment in the Czech Republic. *Agric. For. Meteorol.* **2015**, *202*, 26–38. [[CrossRef](#)]
5. Wang, H.; Vicente-Serrano, S.M.; Tao, F.; Zhang, X.; Wang, P.; Zhang, C.; Chen, Y.; Zhu, D.; El Kenawy, A. Monitoring winter wheat drought threat in Northern China using multiple climate-based drought indices and soil moisture during 2000–2013. *Agric. For. Meteorol.* **2016**, *228*, 1–12. [[CrossRef](#)]
6. Masupha, T.E.; Moeletsi, M.E. Use of standardized precipitation evapotranspiration index to investigate drought relative to maize, in the Luvuvhu River catchment area, South Africa. *Phys. Chem. Earth Parts A/B/C* **2017**, *102*, 1–9. [[CrossRef](#)]
7. Hui-Mean, F.; Yusop, Z.; Yusof, F. Drought analysis and water resource availability using standardized precipitation evapotranspiration index. *Atmos. Res.* **2018**, *201*, 102–115. [[CrossRef](#)]
8. Parsons, D.J.; Rey, D.; Tanguy, M.; Holman, I.P. Regional variations in the link between drought indices and reported agricultural impacts of drought. *Agric. Syst.* **2019**, *173*, 119–129. [[CrossRef](#)]
9. Feng, P.; Wang, B.; Liu, D.L.; Yu, Q. Machine learning-based integration of remotely-sensed drought factors can improve the estimation of agricultural drought in South-Eastern Australia. *Agric. Syst.* **2019**, *173*, 303–316. [[CrossRef](#)]
10. Shen, Y.; Li, S.; Chen, Y.; Qi, Y.; Zhang, S. Estimation of regional irrigation water requirement and water supply risk in the arid region of Northwestern China 1989–2010. *Agric. Water Manag.* **2013**, *128*, 55–64. [[CrossRef](#)]
11. Tanasijevica, L.; Todorovica, M.; Pereirab, L.S.; Pizzigallic, C.; Lionellob, P. Impacts of climate change on olive crop evapotranspiration and irrigation requirements in the Mediterranean region. *Agric. Water Manag.* **2014**, *144*, 54–68. [[CrossRef](#)]
12. Wu, D.; Fang, S.; Li, X.; He, D.; Zhu, Y.; Yang, Z.; Xu, J.; Wu, Y. Spatial-temporal variation in irrigation water requirement for the winter wheat-summer maize rotation system since the 1980s on the North China Plain. *Agric. Water Manag.* **2019**, *214*, 78–86. [[CrossRef](#)]
13. Zhang, Y.; Wang, Y.; Niu, H. Effects of temperature, precipitation and carbon dioxide concentrations on the requirements for crop irrigation water in China under future climate scenarios. *Sci. Total Environ.* **2019**, *656*, 373–387. [[CrossRef](#)] [[PubMed](#)]
14. Yang, J.; Ren, W.; Ouyang, Y.; Feng, G.; Tao, B.; Granger, J.J.; Poudel, K.P. Projection of 21st century irrigation water requirement across the Lower Mississippi Alluvial Valley. *Agric. Water Manag.* **2019**, *217*, 60–72. [[CrossRef](#)]
15. Allen, R.; Pereira, L.S.; Raes, D.; Smith, M. *Crop Evapotranspiration Guidelines for Computing Crop Water Requirements, Irrigation and Drainage Paper 56*; United Nations FAO: Rome, Italy, 1998.
16. Liu, Y.; Wang, L.; Ni, G.H.; Ni, G.; Cong, Z.T. Spatial distribution characteristics of irrigation water requirement for main crops in China. *Trans. CSAE* **2009**, *25*, 6–12. (In Chinese)
17. Facchia, A.; Gharsallah, O.; Corbarib, C.; Masseronia, D.; Mancinib, M.; Gandolfia, C. Determination of maize crop coefficients in humid climate regime using the eddy covariance technique. *Agric. Water Manag.* **2013**, *130*, 131–141. [[CrossRef](#)]
18. Liu, L.; Luo, Y.; He, C.; Lai, J.; Li, X. Roles of the combined irrigation, drainage, and storage of the canal network in improving water reuse in the irrigation districts along the lower Yellow River, China. *J. Hydrol.* **2010**, *391*, 157–174. [[CrossRef](#)]
19. Henan Bureau of Statistics. *Henan Survey Organization National Bureau of Statistic Information Network. Henan Statistical Yearbook*; China Statistics Press: Beijing, China, 1982–2016.
20. Shandong Bureau of Statistics. *Shandong Survey Organization National Bureau of Statistic Information Network. Shandong Statistical Yearbook*; China Statistics Press: Beijing, China, 1982–2016.
21. Liu, Y.; Luo, Y. A consolidated evaluation of the FAO-56 dual crop coefficient approach using the lysimeter data in the North China Plain. *Agric. Water Manag.* **2010**, *97*, 31–40. [[CrossRef](#)]
22. Ma, Y.X.; Zhang, W.; Zhang, L.Z. Cotton water requirement character during recent 30 years in China. *Chin. J. Appl. Ecol.* **2016**, *27*, 1541–1552. (In Chinese)
23. Brouwer, C.; Heibloem, M. *Irrigation Water Management: Irrigation Water Needs. Training Manual*; FAO: Rome, Italy, 1986; pp. 63–68.

24. Liu, Y.; Teixeira, J.; Zhang, H.; Pereira, L.S.; Teixeira, J. Model validation and crop coefficients for irrigation scheduling in the North China plain. *Agric. Water Manag.* **1998**, *36*, 233–246. [[CrossRef](#)]
25. Thornthwaite, C.W. An Approach Toward a Rational Classification of Climate. *Soil Sci.* **1948**, *66*, 77. [[CrossRef](#)]
26. McVicar, T.R.; Roderick, M.L.; Donohue, R.J.; Li, L.T.; Van Niel, T.G.; Thomas, A.; Grieser, J.; Jhajharia, D.; Himri, Y.; Mahowald, N.M.; et al. Global review and synthesis of trends in observed terrestrial near-surface wind speeds: Implications for evaporation. *J. Hydrol.* **2012**, *416*, 182–205. [[CrossRef](#)]
27. Sheffield, J.; Wood, E.F.; Roderick, M.L. Little change in global drought over the past 60 years. *Nature* **2012**, *491*, 435–438. [[CrossRef](#)] [[PubMed](#)]
28. Ming, B.; Guo, Y.Q.; Tao, H.B.; Liu, G.Z.; Li, S.K.; Wang, P. SPEIPM-based research on drought impact on maize yield in North China Plain. *J. Integr. Agric.* **2015**, *14*, 660–669. [[CrossRef](#)]
29. Xu, K.; Yang, D.; Yang, H.; Li, Z.; Qin, Y.; Shen, Y. Spatio-temporal variation of drought in China during 1961–2012: A climatic perspective. *J. Hydrol.* **2015**, *526*, 253–264. [[CrossRef](#)]
30. Li, X.X.; Ju, H.; Liu, Q.; Li, Y.C.; Qin, X.C. Analysis of drought characters based on the SPEI-PM index in Huang-Huai-Hai Plain. *Acta Ecol. Sin.* **2017**, *37*, 2054–2066. (In Chinese)
31. Wang, L.; Yu, H.; Yang, M.; Yang, R.; Gao, R.; Wang, Y. A drought index: The standardized precipitation evapotranspiration runoff index. *J. Hydrol.* **2019**, *571*, 651–668. [[CrossRef](#)]
32. Singh, V.P.; Guo, H.; Yu, F.X. Parameter estimation for 3-parameter log-logistic distribution (LLD3) by Pome. *Stoch. Environ. Res. Risk Assess.* **1993**, *7*, 163–177. [[CrossRef](#)]
33. General Administration of Quality Supervision, Inspection and Quarantine of P.R.C.; Standardization Administration of the P.R.C. *National Standard of People's Republic of China GB/T 20481-2017, Grades of Meteorological Drought*; China Standard Press: Beijing, China, 2017. (In Chinese)
34. Mann, H.B. Non-parametric tests against trend. *Econometrica* **1945**, *13*, 245–259. [[CrossRef](#)]
35. Kendall, M.G. *Rank Correlation Measures*; Charles Griffin: London, UK, 1975.
36. Mitchell, J.M.; Dzerdzeevskii, B.; Flohn, H. *Climate Change*; WHO Technical Note 79; World Meteorological Organization: Geneva, Switzerland, 1966; p. 79.
37. Sen, P.K. Estimates of the regression coefficient based on Kendall's tau. *J. Am. Stat. Assoc.* **1968**, *63*, 1379–1389. [[CrossRef](#)]
38. Raskin, P.; Gleick, P.; Kirshen, P.; Pontius, G.; Strzepek, K. *Comprehensive Assessment of the Freshwater Resources of the World Water Futures: Assessment of Long-Range Patterns and Problems*; Stockholm Environment Institute: Stockholm, Sweden, 1997.
39. Zhang, J.P.; Zhao, Y.X.; Wang, C.Y.; Yang, X.G.; Wang, J. Impact simulation of drought disaster at different developmental stages on winter wheat grain-filling and yield. *Chin. J. Eco Agric.* **2012**, *20*, 1158–1165. (In Chinese) [[CrossRef](#)]
40. Shao, L.W.; Zhang, X.Y.; Chen, S.Y.; Sun, H.Y.; Pei, D. Yield and water use efficiency affected by rainfall, irrigation and maize varieties. *J. Irrig. Drain.* **2009**, *28*, 48–51. (In Chinese)
41. Yu, X.G.; Sun, J.S.; Xiao, J.F.; Liu, Z.G.; Zhang, J.Y. A study on drought indices and lower limit of suitable soil moisture of cotton. *Acta Gossypii Sin.* **1999**, *11*, 35–38. (In Chinese)
42. Pirmoradian, N.; Davatgar, N. Simulating the effects of climatic fluctuations on rice irrigation water requirement using AquaCrop. *Agric. Water Manag.* **2019**, *213*, 97–106. [[CrossRef](#)]
43. Yang, X.; Gao, W.; Shi, Q.; Chen, F.; Chu, Q. Impact of climate change on the water requirement of summer maize in the Huang-Huai-Hai farming region. *Agric. Water Manag.* **2013**, *124*, 20–27. [[CrossRef](#)]
44. Huang, H.P.; Cao, M.M.; Song, J.X.; Han, Y.P.; Chen, S.S. Water budget of main crops during the whole growth period in Huang-Huai-Hai Plain. *J. Arid Land Resour. Environ.* **2015**, *29*, 138–144. (In Chinese)
45. Zhou, Y.P.; Hu, Z.H.; Cui, H.L.; Chen, S.T.; Shi, L.K. Effect of climate change on main crop water requirements in Henan province during 1971–2010. *J. Nanjing Univ. Inf. Science Technol. Nat. Sci. Ed.* **2013**, *5*, 515–521. (In Chinese)
46. Zhang, R.H. *Crop Irrigation Water Demand in the Yellow River Basin under Climate Change Conditions*; Xi'an University of Technology: Xi'an, China, 2019.
47. Li, A.X.; Xiao, H.; Zhou, J.J.; Yang, H.L.; Bao, X.D. Characteristics of spatio-temporal distribution of spring and autumn precipitation in Henan Province. *Clim. Environ. Res.* **2012**, *17*, 884–896. (In Chinese)

48. Xue, C.; Ma, Z.; Hu, C. Spatiotemporal characteristics of drought during summer maize growing season in Huang-Huai-Hai area for recent 40 years. *J. Nat. Disasters* **2016**, *25*, 1–14. (In Chinese)



© 2019 by the authors. Licensee MDPI, Basel, Switzerland. This article is an open access article distributed under the terms and conditions of the Creative Commons Attribution (CC BY) license (<http://creativecommons.org/licenses/by/4.0/>).